TWENTYFIFTH EUROPEAN ROTORCRAFT FORUM

Paper N2

Analysis of riveted joint failure under mixed modes loading

BY

L.PATRONELLI, B.LANGRAND, E.MARKIEWICZ[Y],
E.DELETOMBE, P.DRAZETIC[Y].
ONERA, FRANCE
[Y]UVHC-LAMIH, FRANCE

SEPTEMBER 14-16, 1999
ROME
ITALY

ASSOCIAZIONE INDUSTRIE PER L'AEROSPAZIO, I SISTEMI E LA DIFESA
ASSOCIAZIONE ITALIANA DI AERONAUTICA ED ASTRONAUTICA

25th EUROPEAN ROTORCRAFT FORUM
Rome, Italy - 14th-16th September 1999

« Structures and Materials » N2

L. Patronelli, B. Langrand, E. Deletombe, E. Markiewicz ¥, P. Drazétic ¥
ONERA-Lille, Solid and Damage Mechanics Department, Structural Resistance and Design Section,
5 boulevard Paul Painlevé, Lille 59045, France
¥ Industrial and Human Automatic Control and Mechanical Engineering Laboratory - Mechanical Engineering Research Group (UMR CNRS 8530) - University of Valenciennes, Le Mont Houy, B. P 311, 59304 Valenciennes Cedex, France

Numerous rivets have to be modelled for simulation of framework crashes. For this kind of application, rivets are modelled with equivalent elements. Failure mode of such elements is defined with a mixed shear/tension law. To characterise rivet failure under mixed mode loading, experiments and FE simulation of the ARCAN test procedure are undertaken with a 7050 aluminium alloy countersunk rivet. Results show that both approaches predict well the rivet failure criterion. Moreover FE tools can also resolve design problems of new riveted assemblies more rapidly and cost effectively than experiments. Analytical and optimisation methods are used to identify the parameter of a mathematical failure criterion of the riveted joint. The analytical method is unsatisfactory when compared to the optimisation method.

1. INTRODUCTION

One of the principal interests of commercial aircraft manufacturers is passenger safety in a crash situation. A crash landing with landing gear in means that crash behaviour must be taken into consideration when designing a new aircraft. Frameworks must be improved in terms of acceleration levels and binnacle deformation. Progress in passenger safety implies a better knowledge of non-linear mechanical behaviours (e.g. significant displacement, failure or local dislocation). These complex phenomena were observed and detected in crash tests of frameworks [1-2]. Manufacturers today use numerical tools based on the finite element method [3-4] in order to reduce development costs. It is however impossible to finely model a whole aircraft (computing time being of course too long). FE codes propose equivalent rivet elements which describe mechanical and complex failure modes in aeronautical structures up to a certain point. The method presented here consists in an accurate rivet's material characterisation (Gurson's damage model) which enables one to build up a numerical database and to identify parameters of a macroscopic failure criterion.

To set up a numerical data base, it is necessary to validate data relative to the material damage model. The results of a reference test and relative FE modelling are therefore compared. Rivets are usually characterised by their tension and shear behaviour. Nevertheless riveted joints are often loaded in mixed modes. The problem is to define an experimental process which undertakes pure loading of shear and tension on the one hand and mixed modes loading on the other hand.

The literature has proposed to use and adapt the ARCAN test procedure [5]. Quasi static tests determine an experimental macroscopic failure criterion for a 7050 aluminium alloy countersunk rivet. FE simulations of the ARCAN test are undertaken to validate Gurson's damage model parameters and define a numerical failure criterion. A mathematical model is then identified to interpolate experimental data. The mathematical model's parameters are identified with two different methods : analytical and optimisation procedure. Finally, the aim of this paper is to show that FE simulation characterises failure of riveted joints more rapidly and cost effectively than a purely experimental process. This research is part of a program which concerns the characterisation of riveted assemblies under dynamic behaviour. This is why the explicit FE code Pam-Solid™ has been chosen.

2. EXPERIMENT

2.1. Set up

The ARCAN test procedure [6] mixes and controls shear and tension loading. The global load, F, can be resolved in two components, N (normal) and T (tangential), as a function of the angular position, α (Equation 1).

$$N = F\cos(\alpha) \quad (1a)$$

$$T = F\sin(\alpha) \quad (1b)$$

(for $\alpha = 0°$, a pure tension load is obtained and for $\alpha = 90°$, a pure shear load is obtained)

The ARCAN set up is composed of two disk quarters made in 45SCD6 steel. The specimen is fixed between these two massive elements and is composed of (Figure 1) :

i. two heels made in a Marval hardenable ($\sigma_y = 1800$ MPa),
ii. one 7050 aluminium alloy countersunk rivet.

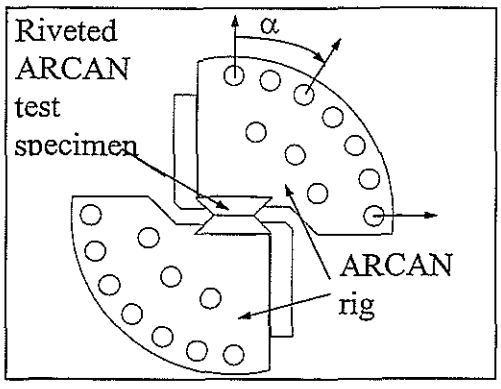

Figure 1. Arcan test procedure.

The riveting process is standardised by geometrical criteria for the strain levels and the volume of the rivet driven head [7]. A special experimental set-up was adapted to rivet the specimen and to calibrate the dimensions of the driven head.

Quasi-static and dynamic tests were performed on a single lap riveted joint specimen [8] and no strain rate influence was measured. Velocity of the riveting and ARCAN test were then taken in the quasi-static range ($V_{imp} = 2$mm/mn). Five configurations of shear/tension load were chosen to define the experimental failure criterion of a riveted joint :

i. pure tension, ($\alpha = 0°$),
ii. mixed shear/tension modes, ($\alpha = \{15°, 30°, 45°\}$),
iii. pure shear, ($\alpha = 90°$).

The riveting and ARCAN tests were performed on a INSTRON 1195 quasi-static tension/compression machine. For each configuration several tests were undertaken to obtain better statistic values. The load was measured by a piezoelectric load cell (Kistler 9070) and the displacement by an extension sensor (Schenck G-Nr 911). A special couple of plates were used to measure the displacement in the load direction (Figure 2).

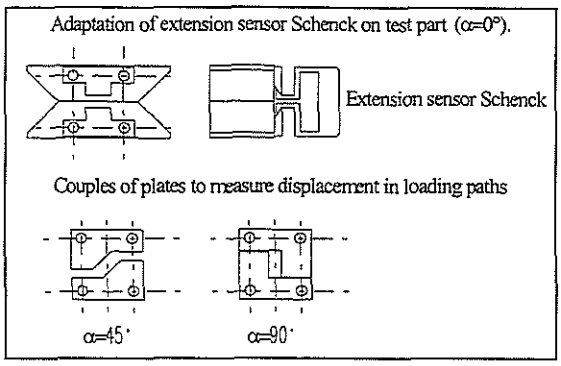

Figure 2. Displacement measurement set up.

2.2. Results

ARCAN test results are given in terms of angular position, α, mean maximum load, F_{max}, mean failure load, F_f, and residual displacement at failure, δ_{res} (Table 1).

Table 1. Experimental results

α (°)	F_{max} (kN)	F_u (kN)	δ_{res}
0	4.450	3.9	0.45
15	4.227	3.4	0.4
30	3.667	3.1	0.4
45	3.276	2.8	0.49
90	2.543	2.0	0.63

There are significant differences between tension and shear pure modes. The angular position influences the global failure mode of the rivet. (Figure 3).

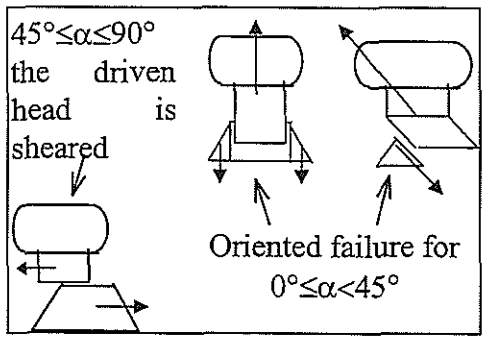

Figure 3. Experimental failure mode of a riveted joint

In pure tension the rivet countersunk head is punched by the rivet shank. This failure mode persists until $\alpha = 30°$ and the failure propagation increase according to this angle. For angular positions between 45° and 90°, the rivet countersunk head is sheared.

Analysis shows that the failure of the rivet is due only to shear stress and that the direction of loading, even in a pure tension load, has no influence. In fact the ratio between maximum tension and shear pure loads (1.75) is comparable to the ratio of the effective shear areas (1.6) (Equation 2). The difference between tension and shear pure loads corresponds to a structural effect due to the rivet geometry.

$$\left(\frac{F_{max}}{S_0}\right)_T \approx \left(\frac{F_{max}}{S_0}\right)_S \approx 200\ MPa$$

Nevertheless equations (1) applied with $F(\alpha) = F_{max}(\alpha)$ define the experimental failure criterion (expressed in terms of N and T forces, Table 2) of the rivet under mixed mode loading.

Table 2. Experimental shear and tension load.

α (°)	T (kN)	N (kN)
0	0	4.450
15	1.094	4.083
30	1.833	3.176
45	2.316	2.316
90	2.543	0

3. F.E.MODEL

FE simulations of the ARCAN test were undertaken to study the capability of explicit FE codes (such as PAM-SOLID™ [9]) to define a rivet failure criterion in numerical ways. To predict this numerical failure criterion material parameters of the elastic-plastic and damage models for 7050 aluminium alloy (rivet material) have to be determined. Parameters of Gurson's damage model have been identified with shear single lap specimens using an inverse method [10]. The interest of ARCAN test modelling is also to evaluate the practical limit of error of the optimised parameters for the 7050 aluminium alloy.

3.1. ARCAN test modelling

In order to correctly reproduce loading and boundary conditions the experimental set-up was modelled completely :

i. both steel disk quarters to orient the load (experimental set-up),
ii. both hardening steel heels (linking the experimental set-up to the rivet),
iii. the rivet itself.

Two rigid bodies were defined with a steel disk quarter and a heel (Figure 4). Each rigid body master node was moved by a rigid wall. Rigid walls were chosen as moving tied infinite planes with infinite mass and finite velocity ($V_{imp} = 0.2$ m/s). Rigid wall definition does not permit a free displacement of the slave node (that is to say the rigid body master node). As the experimental set-up and heel remain in the elastic range they were modelled with elastic solid elements. The rivet was modelled with porous solid elements (type 26).

The contact between the rivet, the punching and the heel was controlled by a self-impacting contact interface with a finite friction ($f = 0.2$). Behaviour of 7050 aluminium alloy is given in terms of Gurson's damage model parameters (q_1, q_2, f_I, f_N, S_N, ε_N, f_C, f_F) (Table 3). Yield stresses of disk quarters (45 SCD 6) and heels (Marval) are 1700 and 1800 MPa respectively.

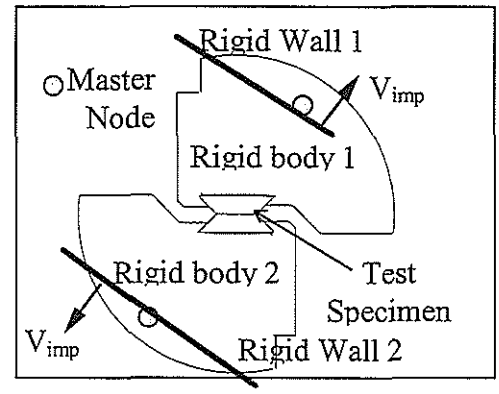

Figure 4. FE modelling.

Table 3. Gurson damage parameters

Type of load	Damage (Gurson model)							
	q_1	q_2	f_I	f_N	S_N	ε_N	f_C	f_F
Crush	for crush load no damage is allowed by Gurson model							
Tension	1.5	1.5	1^{E-07}	0.045	0.075	0.15	0.045	0.055

Residual stresses and strains due to the riveting process were taken into account as initial state of the ARCAN test procedure simulations [11-12] which were performed for $\alpha = \{0°, 30°, 45°, 90°\}$. The FE model was finally made up with 45600 solid elements. The time step is in the order of 10^{-5} ms. Each simulation

was performed on a HP 9000C100 workstation, until failure appeared. The CPU time was in the order of 10 hours. The FE model results and experimental results are compared in terms of the load vs. displacement.

3.2. F.E. results

Table 4 shows F.E. model and experimental results in terms of F_{max}, δ_{res}, N and T. For each configuration the rivet global failure mode (e.g. for $\alpha = 0°$, Figure 5 a-b), as well as the global load vs. displacement response, are correctly predicted by the F.E. model (Figure 6). Comparison of the numerical and experimental failure criterion shows a good correlation (Figure 7). The quality of results proves that Gurson's damage model parameters identified with shear single lap specimens are suitable to characterise the rivet failure criterion on the basis of the ARCAN procedure. On the contrary of a purely experimental procedure, the numerical tool allows to inexpensively refine and complete the failure criterion by the simulation of multiple loading directions.

Table 4. ARCAN results.

α °	Method EXP/MEF	F_{max} kN	δ_{res} mm	N kN	T kN
0	EXP	4.45	0.4	4.45	0
	MEF	4.51	0.35	4.51	0
30	EXP	3.66	0.45	3.17	1.83
	MEF	4.02	0.4	3.48	2.01
45	EXP	3.27	0.5	2.31	2.31
	MEF	3.45	0.45	2.44	2.44
90	EXP	2.54	0.7	0	2.54
	MEF	2.35	0.6	0	2.35

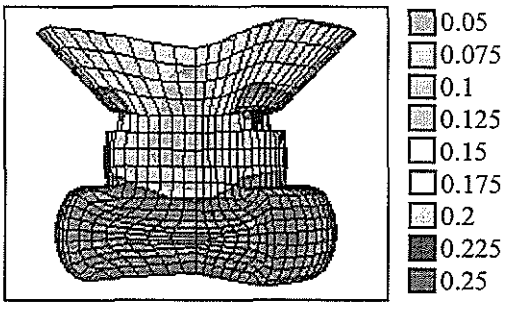

Figure 5a. Equivalent plastic strain (α=0°).

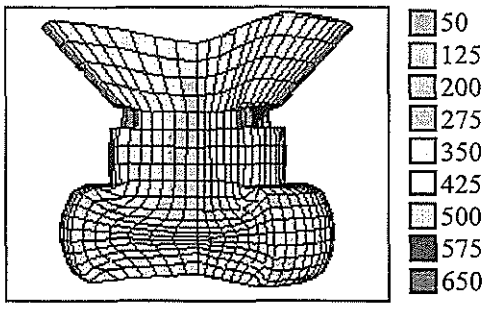

Figure 5b. Equivalent von Mises (MPa, α=0°)

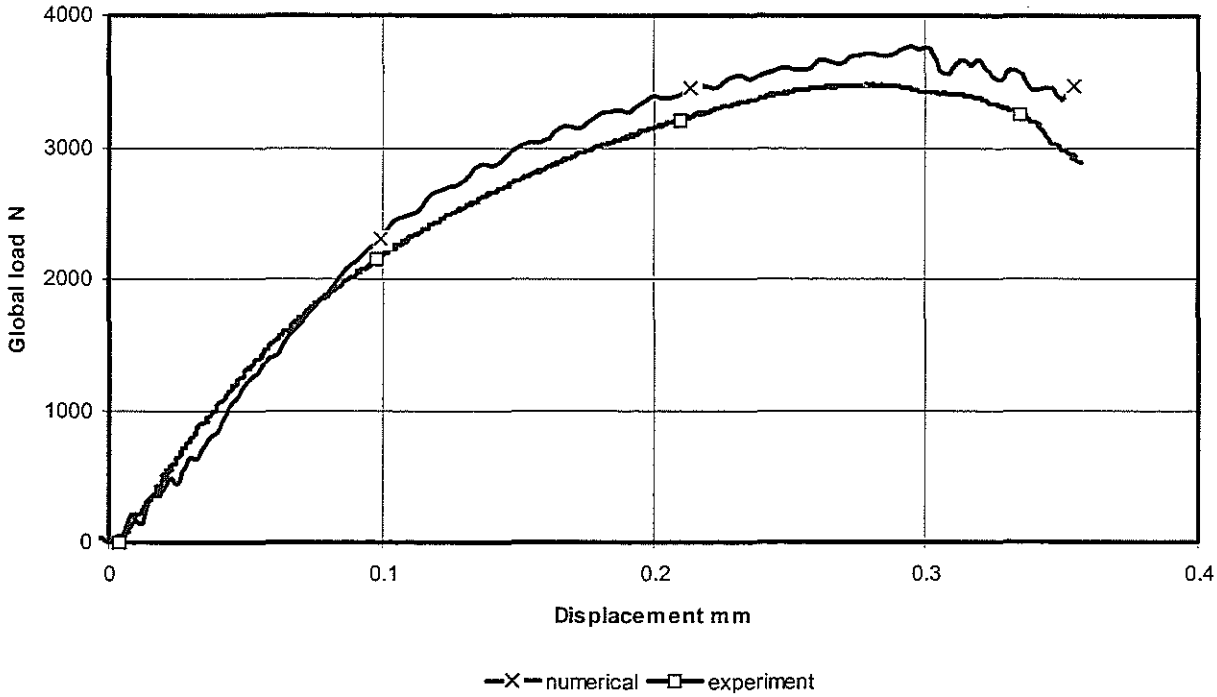

Figure 6. Load vs. displacement diagram (α = 30°)

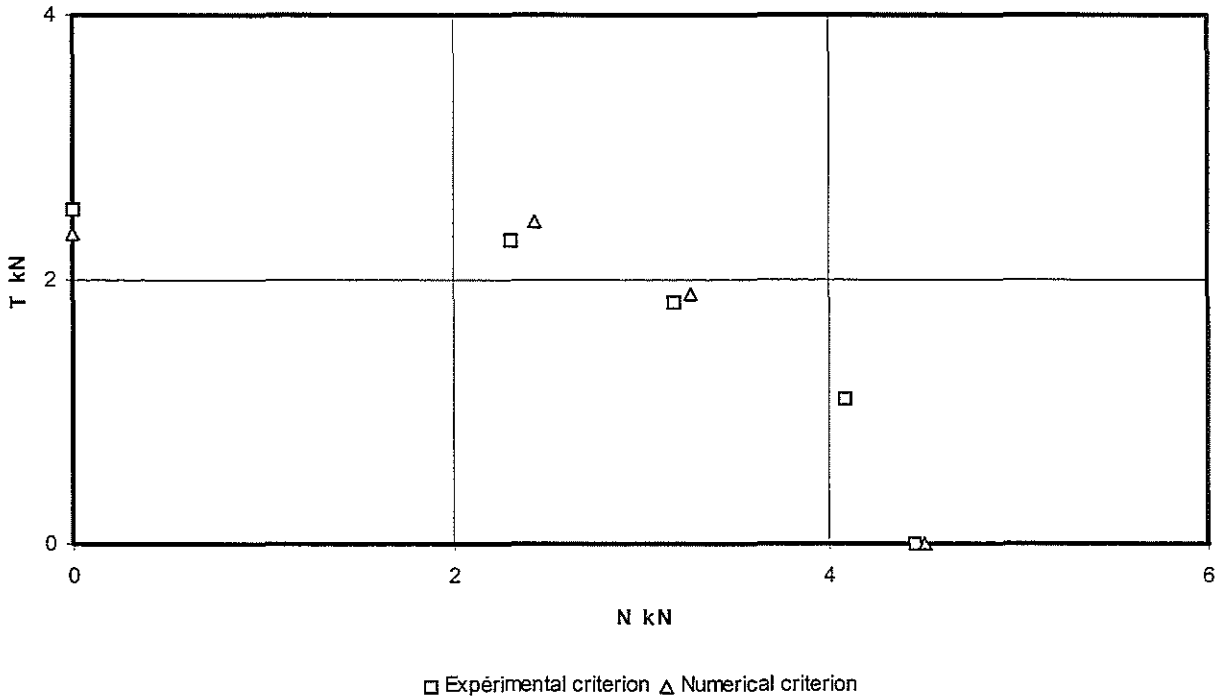

Figure 7. Comparison between experimental and numerical failure criterion.

4. IDENTIFICATION OF THE MACROSCOPIC FAILURE CRITERION

The mathematical model chosen to describe the experimental or numerical failure criterion corresponds to an elliptic formulation (Equation 2).

$$\left(N/N_u\right)^a + \left(T/T_u\right)^b \leq 1 \qquad (2)$$

The initial parameters' vector to identify is $\{N_u, T_u, a, b\}$. N_u and T_u values are directly defined by $\{N(\alpha) \mid \alpha = 0°\}$ and $\{T(\alpha) \mid \alpha = 90°\}$ ($N_u = 4.45$ kN and $T_u = 2.54$ kN). The identification process will therefore concern the reduced parameter vector {a, b}. The simplification a = b is commonly used because of a lack of shear/tension mixed load measurement [13]. With the ARCAN test procedure it is unusual to consider this simplification. The influence of the two hypothesis a = b and a ≠ b on the quality of the identified failure criterion is evaluated.

4.1. Case a = b

With $K_1 = N/N_u$ and $K_2 = T/T_u$, the initial failure criterion model given by equation (2) becomes (3).

$$\left(K_1\right)^a + \left(K_2\right)^a = 1 \tag{3}$$

This equation can not be resolved in a purely analytical way. An approximation can be obtained with a method based on recurrent series and graphic identification. A series is built (equation 5) which converges towards the solution $U_{n+1} = U_n$.

$$U_{n+1} = \frac{ln\left(1 - \left(K_2\right)^{U_n}\right)}{ln\left(K_1\right)} \tag{5}$$

This solution is also the intersection between the two curves defined by equations (6-7) :

$$Y = \frac{ln\left(1 - \left(K_2\right)^{X}\right)}{ln\left(K_1\right)} \tag{6}$$

$$Y = X \tag{7}$$

'a' is determined by just one couple (N,T) which must be taken in the range : $\alpha = \{15°, 30°, 45°\}$ (tension/shear mixed load). Table 5 shows the values obtained for 'a' with $\alpha = \{15°, 30°, 45°\}$ (e.g. $\alpha = 15°$, Figure 8). The analysis of results shows that the value of the parameter 'a' depends on the initial loading way (Figure 9). To improve the solution's stability, the entire experimental database must be considered. This method requires an optimisation tool. The in-house program OPTB2L [14] is used to identify 'a'. The obtained value is a = 2.19 (Figure 10). With this last value the experimental failure criterion is correctly interpolated.

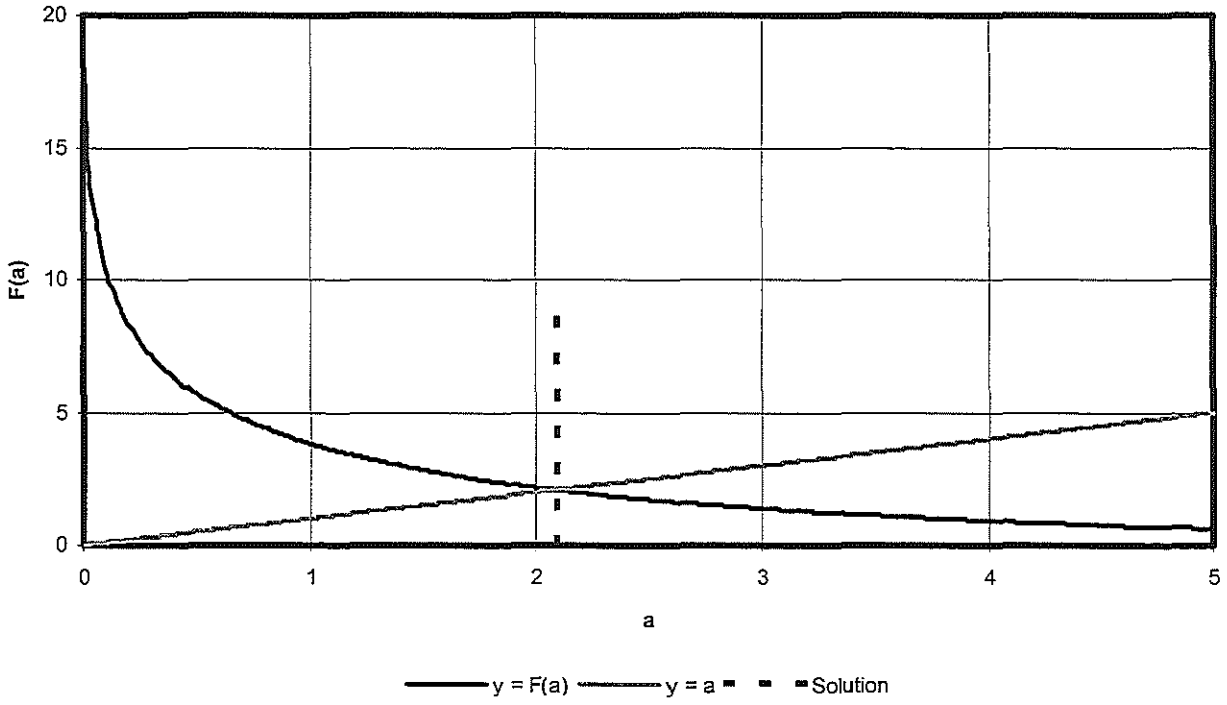

Figure 8. Analytical identification of parameter a (α = 15°).

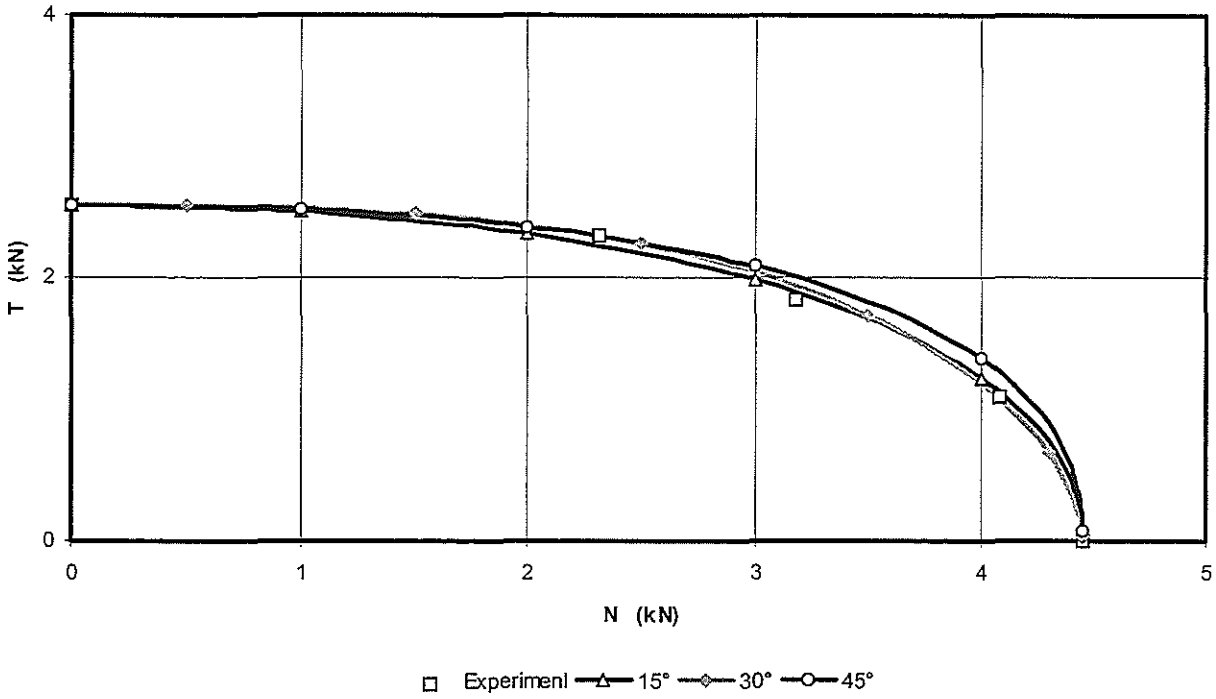

Figure 9. Identified failure criterion by recurrent series method (case a = b).

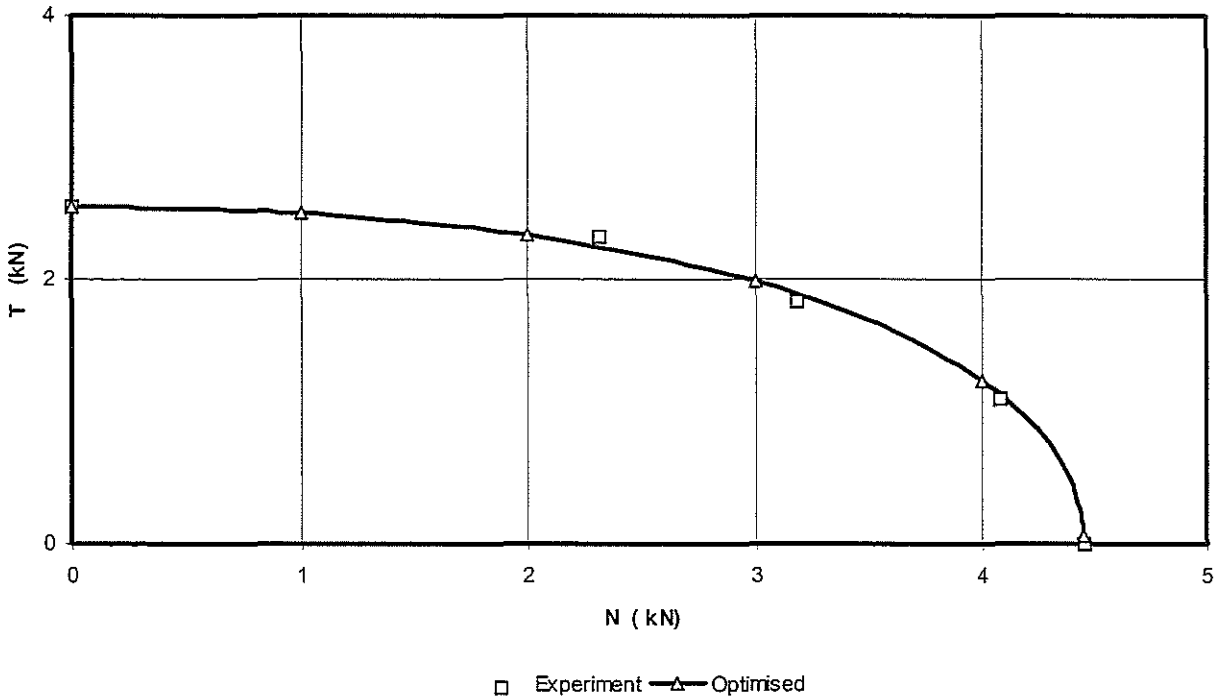

Figure 10. Identified failure criterion with OPTB2L (case a = b).

4.2. Case a≠b

The method based on recurrent series and graphic determination is still the same as in the case a = b. Nevertheless the method of recurrent series requires a couple of experimental points (α_1,α_2). With $K_{i1} = T_i/T_u$ and $K_{i2} = N_i/N_u$ (where i = 1, 2), equations (6-7) become (8-9). The value of the parameter 'a' is found at the

intersection of the curves defined by equations (8) and (9).

$$Y = \frac{ln\left(1-\left(K_{11}\right)^{B(X)}\right)}{ln\left(K_{12}\right)} \qquad (8)$$

where $B(X) = \dfrac{ln\left(1-\left(K_{22}\right)^{X}\right)}{ln\left(K_{21}\right)}$

$$Y = X \qquad (9)$$

The value of the parameter 'b' is directly obtained with B(X) and results are given in Table 6. As in the first case (a = b) the quality of the identified failure criterion is function of the couple of experimental points taken into account to guide the analytical method. With the in-house program OPTB2L the global identification leads to the parameter vector {a, b} = {2.8, 1.8}.

Table 5. Values of parameter a (case a = b).

α (°)	a
15°	2.12
30°	2.085
45°	2.435

Table 6. Values of parameters a and b (case a ≠ b).

couple α (°)	a	b
{15,30}	1.98	2.19
{15,45}	2.85	1.81
{30,45}	3.58	1.08

4.3. Synthesis

Values of $N(\alpha)_{\alpha=0°}$ and $T(\alpha)_{\alpha=90°}$ have defined $N_u = 4.45$ kN and $T_u = 2.54$ kN. An analytical and optimisation method were used to define the value of the vector {a, b}. In both cases (a = b and a ≠ b) the analytical method was very sensitive to the couple of experimental point chosen. Finally it was shown that :

i. the analytical method leads to results equivalent to the optimiser OPTB2L for :
   ⇒ α = 15°, and (a = b),
   ⇒ α = (15°, 45°), and (a ≠ b),
ii. the case (a = b) was as efficient as the case (a ≠ b) for the countersunk rivet and material considered in this study (Figure 11),
iii. parameter vectors defined by the optimiser OPTB2L were :
   ⇒ {Nu, Tu, a, b} = {4.45, 2.54, 2.19, 2.19}, for (a = b),
   ⇒ {Nu, Tu, a, b } = {4.45, 2.54, 2.8, 1.8}, for (a ≠ b).

5. CONCLUSION

This paper deals with the characterisation of a macroscopic failure criterion for a riveted joint under mixed modes. The first part presents in more details the ARCAN test procedure. Experiments are carried out on a countersunk rivet made of a 7050 aluminium alloy. Results show that such an experimental set-up can define the failure criterion of an elementary riveted joint.

In the second part, F.E. modellings of the ARCAN test procedure are undertaken to predict this failure criterion in numerical ways. The practical limit of error of Gurson's damage model (used to describe the damage and failure behaviour of the rivet material) parameters is found for a 7050 aluminium alloy. Results show that the rivet failure criterion is properly predict with this numerical tool. The interest of the F.E. tool is also to resolve design problems related to new riveted assemblies more rapidly and cost effectively than experiments.

The last part is devoted to the identification of a mathematical criterion (usually used to describe the failure behaviour for rivet equivalent elements). The parameters of this criterion are identify by an analytical and an optimisation methods. The optimisation method leads to better results when compared to the analytical one. Moreover with the hypothesis (a = b) the identified failure criterion is as efficiency as the case (a ≠ b) for the rivet and the material considered in this study. Finally, the parameter vector $\underline{z} = \{N_u, T_u, a, b\}$ defined by the self-developed program OPTB2L is : $\underline{z} = \{4.45, 2.54, 2.19, 2.19\}$ for (a = b) hypothesis and $\underline{z} = \{4.45, 2.54, 2.8, 1.8\}$ (a ≠ b).

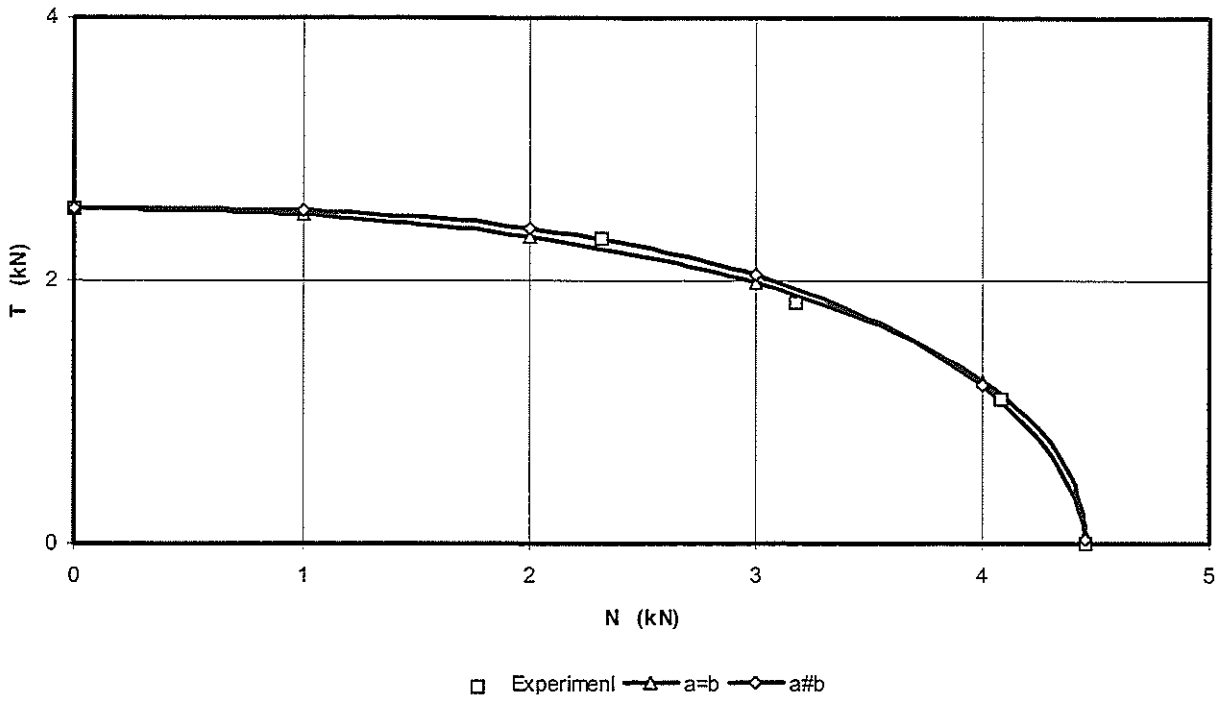

Figure 11. Comparison between cases a = b and a≠ b with OPTB2L failure criterion

Acknowledgement—This research was carried out with an ONERA grant (operation number 98216). The authors are grateful to the ESI Group for the PAM-SOLID™ FE code. The authors also wish to thank the DASSAULT AVIATION Company.

REFERENCES

1 Petitniot, J-L. and Fabis, J. *'CRASH SUR SITE - Etude dynamique d'une maquette structuralement représentative d'un élément de fuselage d'un avion de transport.'*, ONERA-Lille report n°84/48, (1983).

2 Dupriez, F. and Petitniot, J-L. *'Crash test on a 1/3 replica scale model of SA 341 helicopter'*, ONERA-Lille report n°80/05, (1980).

3 Deletombe, E. *'IMT crashworthiness for commercial aircraft. Finite element modelling of joints, plastic buckling and failure - Final report'*, ONERA-Lille report n°96/25, (1996).

4 Deletombe, E. and Malherbe, B. *'Simplification of an aircraft FE model for crashworthiness analysis - Stage 1 - Final report'*, ONERA-Lille report n°97/02, (1997).

5 Arcan, L. Arcan, M. Daniel, M. *'SEM fractography of pure and mixed mode interlaminar fracture in graphite/epoxy composite'*, ASTM Special Technical Publication, Vol. **948**, pp. 41-47, (1987).

6 Gineste, B. *'Assemblage de structure en matériaux composite par stratification d'un élément de liaison. Caractérisation de l'endommagement'*, Thèse de doctorat, École Centrale de Nantes, (1993).

7 US Military standard *'Military standard, preparation for and installation of'*, MIL-STD-403C-14, (1992).

8 Langrand, B. *'Experimental characterisation of 2024-T351 and 7050 aluminium alloys'*, ONERA-Lille report n°97/54, (1997).

9 PAM-SOLID™, *User's manual*, ESI-PSI, (1996).

10 Langrand, B. Deletombe, E. *'Characterisation of Gurson damage model for 7050 aluminium alloy.'*, ONERA-Lille report n°98/13, (1998).

11 Markiewicz, E. Langrand, B. Patronelli, L. et al *'Analysis of the riveting process forming*

mechanisms', Int. J. of Materials and Product Technology, Vol. **13**, N°3-6,pp. 123-145, (1998).

12 Langrand, B. *'Riveted joint embrittlement - Validation of riveting process finite element models'*, ONERA-Lille report n°98/01, (1998).

13 Muller-Bechtel, M. 'Schweifpunktversagen in der FE-crashsimulation', *diplomarbeit in German,* (1994).

14 Langrand, B. Geoffroy, P. Petitniot, J.L. et al *'Constitutive models characterisation for XC48 steel in compression by a parametric identification technique'*, Int. J. of Materials and Product Technology, Vol. **12**, N°4-6, pp. 428-446, (1997).